Available online at www.sciencedirect.com
ScienceDirect
Trans. Nonferrous Met. Soc. China 26(2016) 2770−2783
Transactions of Nonferrous Metals Society of China
www.tnmsc.cn

Sessile drop evaluation of high temperature copper/spinel and slag/spinel interactions

E. de WILDE[1], I. BELLEMANS[1], M. CAMPFORTS[2], M. GUO[3], B. BLANPAIN[3], N. MOELANS[3], K. VERBEKEN[1]

1. Department of Materials Science and Engineering, Ghent University, Technologiepark 903, B-9052 Zwijnaarde (Ghent), Belgium;
2. Umicore R&D, Kasteelstraat 7, B-2250 Olen, Belgium;
3. Department of Materials Engineering, KU Leuven, Kasteelpark Arenberg 44, bus 2450, B-3001 Heverlee (Leuven), Belgium

Received 8 September 2015; accepted 26 February 2016

Abstract: Metal droplets sticking to spinel solids, present in metallurgical slag systems, play an important role in hindering the sedimentation of copper in slags. To understand this phenomenon, the interaction between spinel particles with Cu on one hand and with slag, on the other hand, was evaluated. A dedicated approach was applied, using an industrially relevant synthetic slag system PbO−FeO−SiO_2−CaO−Al_2O_3−Cu_2O−ZnO, pure copper and $MgAl_2O_4$ substrates to represent the industrial slag, the entrained copper droplets and the spinel solids, respectively. Both the copper−$MgAl_2O_4$ and the slag−$MgAl_2O_4$ interaction were studied using sessile drop measurements, combined with an extensive microstructural analysis. Additionally, the effect of time on the slag−$MgAl_2O_4$ interaction was studied using immersion experiments. Copper displayed a non-wetting behaviour on $MgAl_2O_4$, whereas slag displayed a reactive wetting and an interaction layer of $(Mg,Fe,Zn)(Al,Fe)_2O_4$ spinel was formed at the interface, which was also observed in the immersion experiments. Moreover, the diffusion of MgO and Al_2O_3 from the spinel substrate into the slag droplets was noted.

Key words: sessile drop; copper; spinel; slag

1 Introduction

Slags play an essential role in pyrometallurgical processes, for the elimination of unwanted impurities or acting as collectors for specific groups of metals. Therefore, a decantation step is often used in pyrometallurgical processes, allowing the phase separation between matte or metal and slag. Although desirable, these phase separations are not perfect, therefore industrial copper plants suffer from metal losses in slags, which confines the overall metal recovery [1]. To minimize these metal losses and improve the efficiencies of the industrial plants, it is essential to determine the origin and mechanisms behind these metal losses.

Based on extensive research performed on copper losses, it is currently well accepted that copper losses in slags are attributed to both mechanical entrainment of copper-containing droplets and chemical copper losses [2−4]. Chemical copper losses are caused by the dissolution of copper as sulphide and oxide for primary copper production and mainly in its oxide form for secondary copper production. This type of losses is intrinsic to pyrometallurgical processes and is determined by the thermodynamic parameters of the system such as the temperature, the composition of the slag and the matte phase [3,5−7], the oxygen partial pressure [3,5−7], the kinetics and the chemical activity of the metal [3].

Mechanically entrained copper is defined as entrapped or floating unsettled droplets. In primary copper production, both matte and metallic droplets occur, while in secondary copper production, these losses are mainly under the form of metallic copper droplets. Mechanically entrained droplets are ascribed to a variety of causes. The first important cause is the dispersion of copper sulphide or copper, which precipitates due to a local change of the solubility in the slag, for example, in zones with different oxygen partial pressures or a lower

Corresponding author: E. de WILDE; Tel: +32-9-331-04-41; E-mail: evelien.dewilde@gmail.com
DOI: 10.1016/S1003-6326(16)64344-3

temperature due to inhomogeneity of the process [8]. The second important source is entrained matte or metal, originating from gas-producing reactions dispersing metal into the slag. The resulting SO_2 bubbles nucleate at the bottom of the furnace and can elevate a surface film of matte or metal to the slag above [8−10]. Mechanical losses can also occur from operational procedures typically performed in pyrometallurgical processes like tapping or charging. Mechanical entrainment during tapping can originate due to the rise of a denser layer, which can happen while flowing around obstructions in the vessel [2]. The physical dispersion of matte or metal into the slag by mixing can originate from several causes such as gas injections, pouring one phase into the other or the presence of turbulence [2,11]. The above-mentioned sources have been examined profoundly and reported in literature. Additionally, the penetration of metallic copper into refractory can lead to metal losses [12]. There is, however, the fifth possible cause of mechanically entrained metal droplets, namely the attachment of droplets to solids in the slag, which obstructs their decantation. In copper industry, these solids are often identified to have a spinel structure. Notwithstanding the fact that the phenomenon has been reported by IP and TOGURI [8] and ANDREWS [11], and was observed by DE WILDE et al [13], so far limited industrial or experimental data concerning this phenomenon were reported. A prerequisite to further improve the phase separation in pyrometallurgical processes is a better understanding of the interactions among the three different phases involved (metal droplet, solids and slag).

Different methodologies have been applied to studying metal losses in slags. However, little attention has been given to the phenomenon of sticking droplets and more specifically to the spinel–copper and spinel–slag interactions. The wetting behaviour between metals and oxides has been studied frequently, as summarized by EUSTATHOPOULOS and DREVET [14]. In most cases, a distinction is made between reactive and non-reactive systems. Non-reactive systems reach equilibrium in less than 0.1 s for millimetre sized droplets while slower spreading kinetics is a strong indication of the presence of interfacial reactions [15−17]. With respect to the specific wettability of metals on spinel substrates, KOZLOVA and SUVOROV [18] and FUKAMI et al [19] performed experimental studies on the wettability of iron on $MgAl_2O_4$ spinel substrates, but no data have been found on the wetting of copper on spinel substrates specifically.

Wettability between slags and spinels has been studied in the frame of the study of inclusion removal in steel refining on one hand, and the effect of the slag attack on refractories on the other hand. ABDEYZDAN et al [20] investigated the wettability of $CaO-Al_2O_3-SiO_2-MgO$ slag on $MgAl_2O_4$ spinels, and concluded that the slag showed a fast decrease of the contact angle during the first second, after which a plateau is reached for longer time [20]. Even at shorter timescales, slag reaction and penetration were observed. DONALD et al [21] studied the interactions between fayalite slags and synthetic spinels, representing refractory materials. Interfacial reaction products and dissolution of various refractory compounds into the slags were observed. TRAN et al [22] studied the wetting between magnesia spinel bonded refractory and slag, revealing the effect of the Fe-content in the slag and temperature. Nevertheless, previous research focused on fayalite-type slags. Studies on the wetting behaviour between spinel and PbO-based slag have, to our knowledge, not been published before. Moreover, the sessile drop technique was not used before studying the losses due to the attachment of copper droplets to spinel solids in a slag phase.

This present study focuses on the interaction between spinel substrates and slag or copper, respectively. In this research, $MgAl_2O_4$ was chosen to represent the spinel phase, as this is one of the most stable spinel powders. A synthetic industrially relevant PbO-based slag was used ($PbO-FeO-SiO_2-CaO-Al_2O_3-Cu_2O-ZnO$). The (dynamic) wetting behaviour of spinel/copper and spinel/slag has been investigated combined with a detailed microstructural analysis. In addition, the evolution in time of the interaction between spinel and slag has been studied by variation of the immersion time of spinel substrates in the slag.

2 Experimental

2.1 Production of slag system

The slag was produced by melting oxides of appropriate quantities. Therefore, an appropriate slag composition was selected to obtain a spinel saturated single phase slag based on thermodynamic calculations using FactSage 6.4 thermochemical package (FACT and FT Oxid database). The final targeted slag composition is shown in Table 1. CaO was added as limestone and FeO was added as a combination of metallic iron and hematite. 400 g of the targeted composition was weighed, mixed and transferred in an Al_2O_3 crucible (270 mL). The Al_2O_3 crucible, surrounded by a protective SiC crucible, was heated in an inductive furnace (Indutherm, MU3000) up to a temperature of 800 °C, while a protective N_2 atmosphere was established above the slag. At 800 °C, the N_2 atmosphere was replaced by CO/air mixture with a volume ratio of 1 to 2.44, corresponding to an oxygen partial pressure (p_{O_2}) of 10^{-2} Pa, with a total flow rate of 60 L/h, which was kept constant during the remainder of the experiment.

Subsequently, the slag was heated to 1200 °C and kept 30 min in order to melt all components. N_2 (60 L/h) was bubbled through the slag in order to homogenize the slag. The induction furnace was kept for 150 min at 1200 °C to allow the system to equilibrate. Subsequently, all slags were quenched using a cold sampling bar, which were directly cooled fast in water and then dried in a dry chamber at 150 °C.

Table 1 Targeted synthetic slag composition based on thermodynamic FactSage calculations (mass fraction, %)

ZnO	PbO	SiO_2	Al_2O_3	Cu	CaO	FeO
6.49	39.33	13.76	7.25	3.93	9.83	19.41

A representative sample of the slag after equilibration was embedded in epoxy resin, ground and polished using 9 μm and 3 μm diamond pastes. The sample was analyzed using light optical microscopy (LOM, Keyence VHX-S90BE, LOM) and electron probe microanalysis, using the backscattered electron microscopy mode (BSE, EPMA, JEOL JXA-8530F). For the latter, the sample was coated with a conducting carbon layer.

Subsequently, the composition of the different phases was analyzed using a fully quantitative EPMA-WDS (JEOL JXA−8530F) system, applying an acceleration voltage of 15 kV and a probe current of 15 nA. The oxygen contents of the slag phase and spinel particles were not measured directly; instead the oxidation state of the element was selected a priori. Although both Fe^{2+} and Fe^{3+} can be present, for the sake of clarity, only FeO was shown to be present in both the slag phase and spinel phase. The composition of the copper alloy droplets in the slag system was measured in the elemental state.

2.2 Spinel preparation

The $MgAl_2O_4$ substrates were produced using spark plasma sintering equipment (SPS, type HP D25/1, FCT system Rauenstein, Germany, equipped with a 250 kN uniaxial press), using the same procedure as already described in our previous work [13,23,24]. The $MgAl_2O_4$ powders (Sigma Aldrich, magnesium aluminate, spinel nano powder, <50 nm particle size) were sintered at a temperature of 1300 °C under a load of 60 MPa. The sintered spinel plates were subsequently annealed at 1000 °C for 3 h and in a final step polished to a mirror finish using 9 μm, 3 μm and 1 μm diamond pastes, respectively. A Talsurf profilometer was used to determine the surface roughness. The roughness parameter has an average value of (0.19±0.08) μm. The spinel phase was confirmed by XRD analysis, while some additional small corundum peaks were present in the XRD pattern as well. A more detailed description on the sintering process was given in our previous work [23].

2.3 Sessile drop experiments

2.3.1 Confocal scanning laser microscopy sessile drop set-up

The interaction between $MgAl_2O_4$ and copper or slag was studied using a confocal scanning laser microscopy set-up (CSLM, Lasertec 1LM21- SVF17SP) with an infrared heating furnace. The infrared heating furnace allowed fast heating and cooling in a gastight ellipsoidal chamber in which a 1.5 kW halogen lamp was placed in the lower focus point and the observed sample was positioned in the second confocal point. For this, the ellipsoidal chamber was coated with Au to reflect the light from the halogen lamp to the sample. A programmable PID controller controlled the temperature, read from a type B (Pt−Rh) thermocouple, which was integrated into the sample holder. As described in previous work [23,25], an extra window was placed at the side of the heating chamber, combined with a camera (Ganz ZC-F10C3), which was placed on the same height, allowing to monitor the sessile drop experiment. An oxygen gas analyser was installed in the gas outlet to monitor the p_{O_2} (Cambridge sensotec LTD, Rapidox 2100) [24,26].

2.3.2 Sessile drop experiments

Sessile drop experiments were performed using pure copper or slag droplets on $MgAl_2O_4$ substrates. The experiments were performed under a protective Ar atmosphere. (99.999% pure, $x(O_2)<1\times10^{-6}$). The $MgAl_2O_4$ substrate was cleaned ultrasonically in acetone. The copper was etched using a 1:1 H_2O:HCl solution, to remove the outer copper oxide layer. The $MgAl_2O_4$ substrate was placed on the sample holder and levelled carefully. Subsequently, copper or slag was placed on the substrate and the heating chamber was closed and flushed three times with Ar. The temperature was increased up to 300 °C, with a heating rate of 50 °C/min. After 1 min, the temperature was increased up to 900 °C, with a heating rate of 200 °C/min. After 1 min at 900 °C, the temperature was again increased until 1250 °C (200 °C/min), which was further maintained for 10 min. Finally, the sample was cooled down with a cooling rate of 500 °C/min. The complete interaction between substrate and molten droplet was monitored. The contact angle was defined using the low bond axisymmetric drop shape analysis plug-in for the Image J software, which is based on the fitting of the Young−Laplace equation to the shape of the droplet [27].

The average masses of slag and copper during the sessile drop experiments were 0.0175 g and 0.022 g, respectively. Each experiment has been repeated multiple times to ensure the reproducibility of the observations.

The p_{O_2} value during the experiments was between 6.5 and 7.5 Pa.

The obtained sessile drop samples were embedded (Technovit 4000 powder and liquid), ground until the cross section between the spinel substrate and copper or slag became visible and then polished using 9, 3 and 1 μm diamond paste. Samples were analyzed using LOM and BSE (EPMA). The latter was combined with WDS analysis (EPMA, acceleration voltage=15 kV; probe current=15 nA), in order to measure phase compositions, as explained in Section 2.1.

2.4 Study of time effect on slag−spinel interaction

2.4.1 Methodology

$MgAl_2O_4$ substrates were immersed in the slag for certain interaction time. The spinel substrates were produced using the procedure described in Section 2.2. Slag with a composition as shown in Table 1 was melted in an induction furnace under identical experimental conditions as described in Section 2.1. Prior to immersion of the substrate in the slag, the substrate was heated in the hot zone of the furnace to avoid the slag from cooling down when it would be in direct contact with a cold substrate. Subsequently, the $MgAl_2O_4$ substrates were immersed in the slag for 10 s, 30 s, 1 min and 3 min, respectively. Consequently, the substrate and the attached slag were quenched in water and dried in the dry chamber at 150 °C.

2.4.2 Characterization and analysis

After immersion in the slag and quenching, the $MgAl_2O_4$ substrates were embedded (Technovit 4000 powder and liquid), ground until the interface between the $MgAl_2O_4$ substrate and the slag became visible and finally polished using 9, 3 and 1 μm diamond paste, respectively. The resulting samples were analyzed using LOM and BSE. WDS-line scans (EPMA) were performed at the interface of each sample, as specified in Section 2.1. (acceleration voltage=15 kV; probe current= 15 nA)

3 Results

3.1 Microstructural analysis of equilibrated slag system

The microstructure of the slag phase after 150 min equilibration, which was used for the sessile drop experiment and the immersion experiment, can be observed in Fig. 1. Three phases are present: slag (SL), spinel (SP) and copper droplets (Cu-dr). Some of these droplets stick to spinel particles, as can be clearly seen in Fig. 1(b). The presence of these three phases is consistent with the results from thermodynamic FactSage calculation. WDS analysis has been performed on the present phases and the resulting values are given in Table 2. Additionally, the theoretical compositions, obtained from the preliminary FactSage calculations for the considered experimental conditions (1200 °C, $p_{O_2}=10^{-2}$ Pa; FTOxid and FactPS database) are also given in Table 2. The theoretical amount of Fe_2O_3 was recalculated as FeO. A good similarity is observed between the predicted

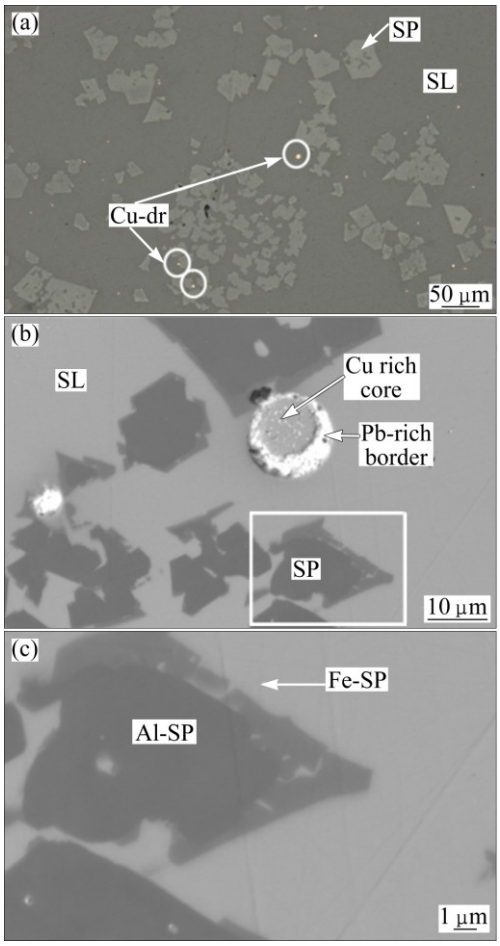

Fig. 1 LOM (a) and BSE (b, c) images of quenched slag obtained after 150 min equilibration (SP—Spinel; SL—Slag; Cu-dr—Copper alloy droplets; Al-SP—Al-rich spinel phase; Fe-SP—Fe-rich spinel phase)

Table 2 WDS analysis of slag, Fe-rich spinel phase and Al-rich spinel phase and compositions of spinel and slag expected based on FactSage thermodynamic calculations (mass fraction, %)

Slag	Al_2O_3	'FeO'	Cu_2O	CaO	ZnO	PbO	SiO_2
Slag (FactSage)	7.1	13.6	4.8	10	5.8	42.8	15
Slag	7.1	16.1	1.3	8.7	5.5	36.4	25.7
Spinel (FactSage)	14.2	74.4	0	0	11.34	0	0
Al-rich spinel	36.9	39.7	0	0	22.5	0.1	0.2
Fe-rich spinel	17.7	63.6	0.1	0	14.3	0.3	0.4

and obtained slag composition; however, a lower amount of Cu_2O is present. The latter can be attributed to the fact that there is still metallic copper present in our system under the form of small entrained metallic copper alloy droplets and a copper layer at the bottom of the crucible. Based on the Factsage calculations, no metallic copper would be expected. This dissimilarity can be attributed to the fact that Factsage assumes ideal mixing of all components, while within the experiment the copper settled down. Furthermore, it can be assumed that after 3 h, no thermodynamic equilibrium was reached yet. The spinel solids result from the three spinel forming components in the slag, namely Al_2O_3, FeO and ZnO and consist of two phases: an Al-rich spinel phase in the core (Al-SP) and an Fe-rich spinel phase at the border (Fe-SP) (Fig. 1(c)). Some spinel particles completely consist of the Fe-rich spinel phase. Based on FactSage calculations, the Fe-rich spinel is the equilibrium phase at 1200 °C. As it is always the Fe-rich spinel phase which is in direct contact and equilibrium with the slag system, focus will be put on the Fe-rich spinel phase.

The WDS analysis of the copper alloy droplets is summarized in Table 3. For the present experimental conditions, these are Cu−Pb droplets with a Pb-rich border and a Cu-rich core, as indicated with arrows in Fig. 1. This observation can be ascribed to the fact that quenching requires a certain, though limited, time which appears to be sufficient to induce a phase separation between Cu and Pb, as a result of the very limited solubility of Cu and Pb at lower temperatures.

Table 3 WDS analysis of Cu-rich core and Pb-rich border of observed Cu−Pb alloy droplets (mass fraction, %)

Droplet	O	Al	Fe	Cu	Ca	Zn	Pb
Cu-rich core	0.7	0	1.5	95	0	0.5	1.2
Pb-rich border	3.4	0	1.4	1.9	0.1	0.9	92.3

3.2 Spinel−copper interaction: sessile drop experiment

Figure 2 illustrates the wetting behaviour of copper on the $MgAl_2O_4$ substrate as a result of the heating of the materials to a temperature of 1250°C and keeping it at this temperature for 10 min under a protective argon atmosphere. The evolution of the contact angle as a function of time is presented in Fig. 3. A clear non-wetting behaviour with a nearly constant contact angle is observed when the sample is kept at 1250 °C. These small variations in the measured contact angle are within the experimental error of the image analysis software program.

The cross-section of the copper droplet on the $MgAl_2O_4$ spinel was studied using BSE images and by WDS analysis. Based on the results, no indications are found for chemical interactions occurring during the experiments.

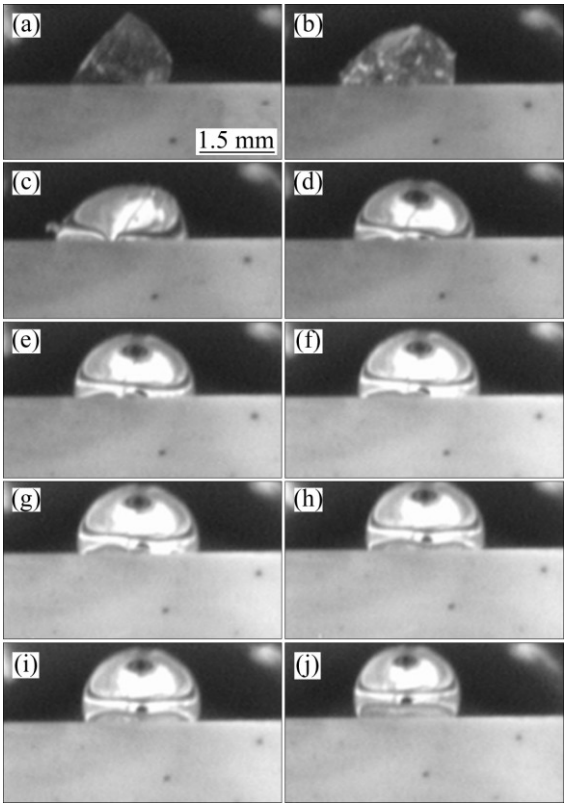

Fig. 2 Melting and wetting behaviour of copper on $MgAl_2O_4$: (a) Before melt; (b) t_{melt}; (c) t_{melt}+5 s; (d) t_{melt}+10 s; (e) t_{melt}+30 s; (f) t_{melt}+100 s; (g) t_{melt}+172 s, T=1250 °C; (h) 120 s, T=1250 °C; (i) 240 s, T=1250 °C; (j) 480 s, T=1250 °C

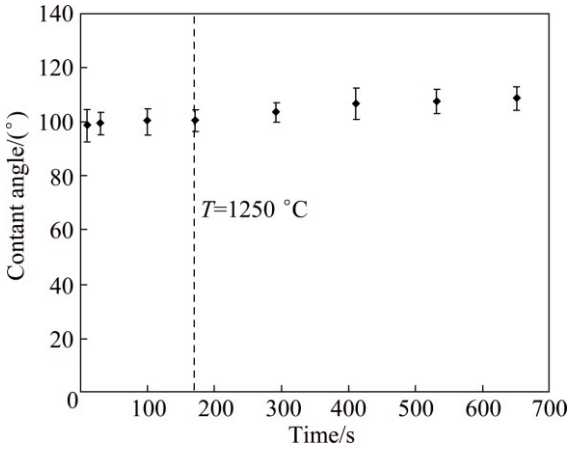

Fig. 3 Evolution of contact angle of pure copper droplet on $MgAl_2O_4$ substrate as function of interaction time (The start of copper melting was taken as origin of the x-axis, i.e. time scale (t_0=t_{melt}))

3.3 Spinel−slag interaction

3.3.1 Wetting behaviour

The wetting behaviour of the synthetic PbO-based slag on the $MgAl_2O_4$ spinel substrate is illustrated in

Fig. 4. The start of slag-melting was taken as the origin of the *x*-axis, i.e., the time-scale. After 100 s, the molten slag obtains a droplet shape, and from that point on contact angles are determined. The corresponding evolution of the contact angle between the slag and the spinel substrate is shown in Fig. 5. Directly after melting, the liquid drop spreads out on the substrate within a couple of minutes while the temperature is increasing up to 1250 °C. A clear significant decrease of the contact angle is observed. Once the maximum temperature is reached, no further significant changes in the contact angle are observed.

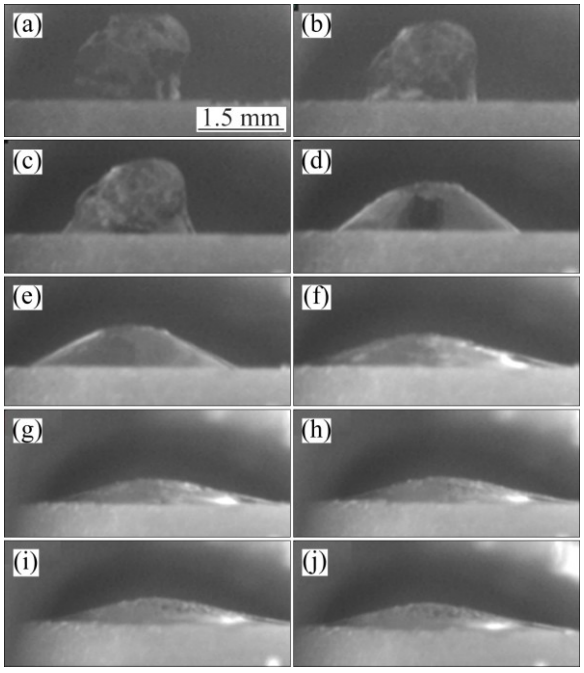

Fig. 4 Melting and wetting behaviour of synthetic PbO−FeO−SiO_2−CaO−Al_2O_3−Cu_2O−ZnO slag on $MgAl_2O_4$ substrate: (a) Before melting; (b) t_{melt}; (c) t_{melt}+60 s; (d) t_{melt}+90 s; (e) t_{melt}+120 s; (f) t_{melt}+180 s; (g) t_{melt}+283 s, T=1250 °C; (h) 200 s, T=1250 °C; (i) 400 s, T=1250 °C; (j) 500 s, T=1250 °C

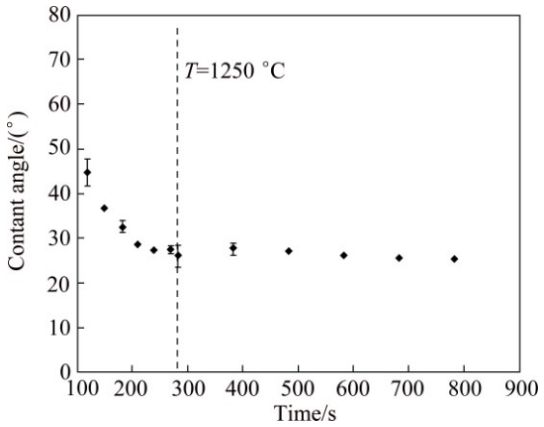

Fig. 5 Evolution of contact angle between slag and $MgAl_2O_4$ substrate as function of interaction time (The start of slag-melting was taken as the origin of the *x*-axis, i.e., the time scale (t_0=t_{melt}). As the slag obtained a droplet shape after 100 s, contact angles are plotted starting from that point)

3.3.2 Microstructural analysis

Figure 6 shows the microstructure of the complete cross-section of the slag−spinel sessile drop sample. Based on the microstructure, the cross-section can be roughly subdivided into four different zones as indicated in Fig. 6: the $MgAl_2O_4$ substrate, an interaction layer at slag−$MgAl_2O_4$ interface, a lower slag layer containing smaller spinel particles and very small black solids, marked with white circles, and the upper slag layer containing larger spinel particles, with a similar microstructure as the slag before the sessile drop experiment.

A detailed image of the interface between the spinel substrate and the slag droplet (zone *b*) is shown in Fig. 7. A WDS-mapping of all present elements in the same area is shown in Fig. 8. The formation of a clear interaction layer along the interface can be observed. This interaction layer consists of a very dense layer close to the spinel substrate which evolves to a layer of densely packed spinel particles with slag in between, further away from the spinel substrate, as indicated in Fig. 7.

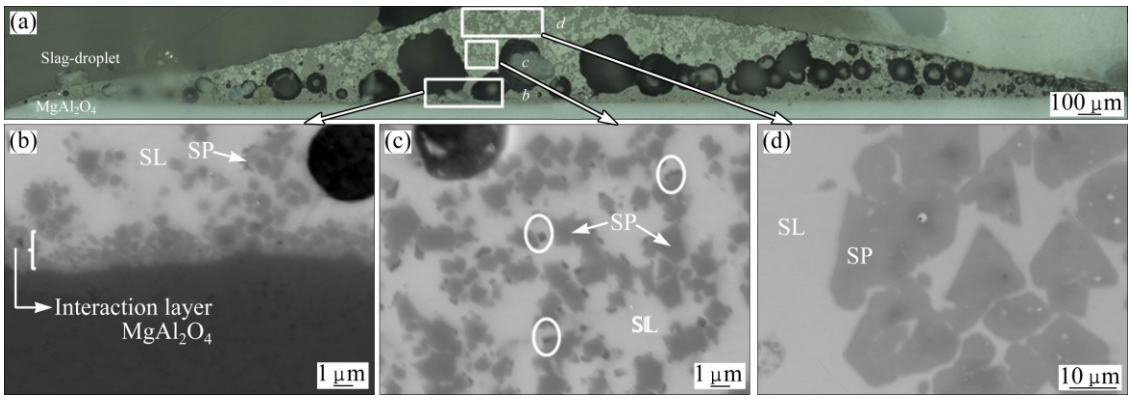

Fig. 6 General overview of complete cross-section between slag and $MgAl_2O_4$ substrate obtained by LOM, with subdivision in four different zones: (a) $MgAl_2O_4$ substrate; (b) Interaction layer at slag−$MgAl_2O_4$ interface; (c) Lower slag layer containing very small black solids marked with white circles; (d) Upper slag layer containing bigger spinel particles

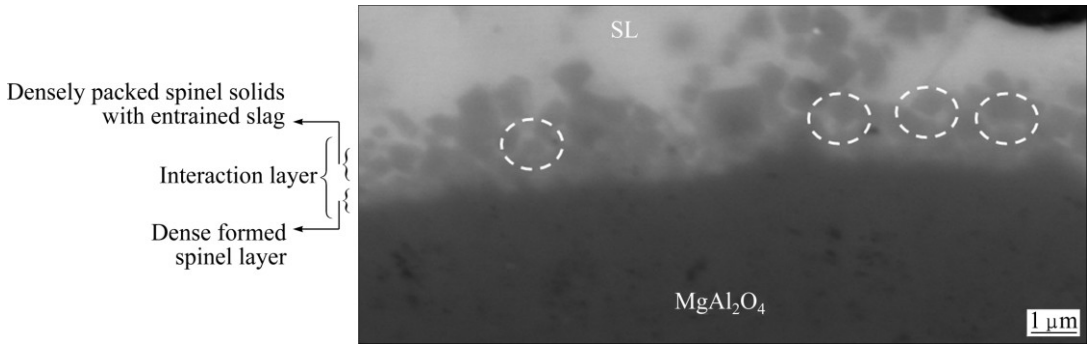

Fig. 7 Detailed BSE image of interaction layer at $MgAl_2O_4$−slag interface in sessile drop sample (This interaction layer can be roughly subdivided into two zones: a dense spinel layer next to the $MgAl_2O_4$ substrate and a densely packed layer of spinel solids with entrained slag on top

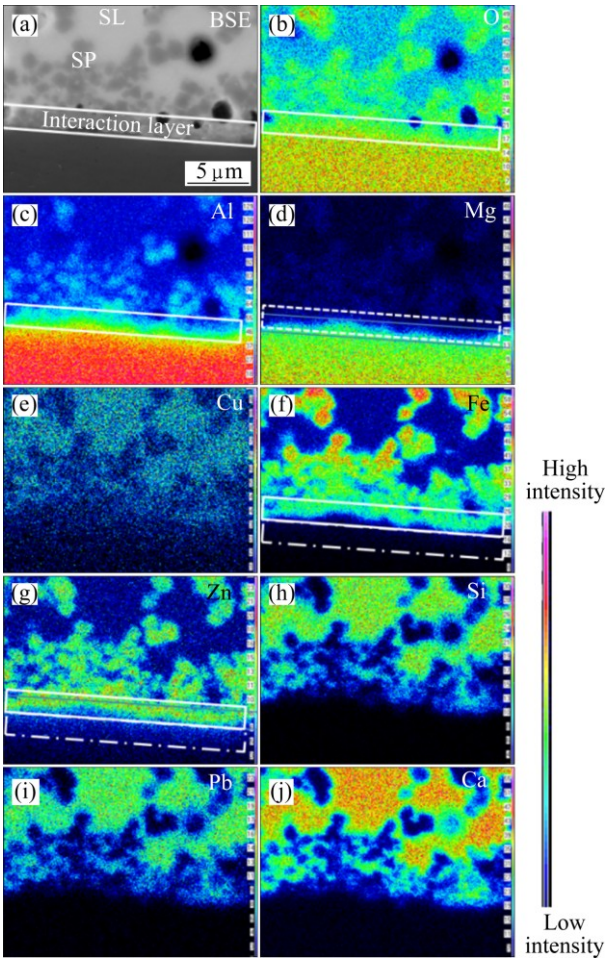

Fig. 8 WDS elemental mapping of slag−$MgAl_2O_4$ interface, indicating presence of interaction layer and possible diffusion of Zn and Fe at upper part of $MgAl_2O_4$ substrate, indicated by dotted frame

Quantitative WDS analysis was performed by EPMA, and the results are summarized in Table 4. The interaction layer of the slag, near the slag−spinel interface was determined to be $(Mg,Fe,Zn)(Al,Fe)_2O_4$ and consisted mainly of Al_2O_3 and MgO, combined with ZnO, Fe_2O_3 and FeO present in the slag. The

Table 4 WDS analysis of interaction layer, slag phase and spinel solids localized above interface and $MgAl_2O_4$ substrate close to interface (zone *b*) (The listed compositions presented are an average value of points measured throughout the whole interface)

Sample	*w*/%							
	Al_2O_3	MgO	'FeO'	Cu_2O	CaO	ZnO	PbO	SiO_2
Upper part $MgAl_2O_4$ substrate	74	22.4	0.52	0.1	0.8	0.8	0	0
Interaction layer	66.9	20.8	3.3	0.4	0.06	7.6	0.07	0.1
Spinel solids in slag	47.5	9.7	20.5	0.4	0.6	19.7	1.6	1.9
Slag	12.7	1.1	6.2	1.7	20.8	1.5	30.5	36.6

composition varies through the interaction layer, which is seen in the elemental Fe, Zn, Mg and Al mappings (Fig. 8). Close to the spinel substrate Mg and Al are dominant, while closer to the slag phase the spinel forming elements (Fe, Zn) present in the slag become more prominent. On the elemental mappings of Fe and Zn, it seems that Fe and Zn are diffused into the upper layer of the $MgAl_2O_4$ substrate. However, the gradient in composition seen on the elemental maps could also be due to an interference with the interaction layer. No indications for diffusion of the main slag forming elements (Pb, Si, Ca, Cu) towards the spinel substrate are observed. The WDS analysis indicates a 5% increase of Al_2O_3 present in the slag as compared with the slag-composition before the sessile drop experiment (Table 2), indicating that Al_2O_3 dissolution into the slag has taken place.

Above the interaction layer, a lower slag layer containing small spinel solids is present, as shown in Fig. 6(c). EPMA−WDS analysis performed on the spinel solids and the slag phase are summarized in Table 5. The

spinel solids consist of Al_2O_3, MgO, FeO and Fe_2O_3. Compared with the spinel solids next to the interaction layer, the spinel solids in this zone are enriched in FeO–Fe_2O_3 and depleted in Al_2O_3 and MgO. Some very small black solids are present on the BSE image and seem to have formed on the spinel solids, as indicated in Fig. 6. However, due to their very small size, no good elemental analysis is possible because of the interference with the surrounding slag phase and adjacent spinel solids.

Table 5 WDS analysis of slag phase and spinel solids in intermediate slag layer of $MgAl_2O_4$−slag sessile drop sample (mass fraction, %)

Sample	Al_2O_3	MgO	'FeO'	Cu_2O	CaO	ZnO	PbO	SiO_2
Slag	13.7	1.3	6.6	1.7	10.6	1.7	29	35.4
Spinel	39	6.4	31	0.5	0.6	19.6	1.9	2.3

At the upper part of the droplet, a slag phase is present with a similar microstructure as the unreacted slag system (Fig. 6(d)). Quantitative WDS analysis of the spinel particles and the slag are given in Table 6. The EPMA−WDS results indicate that the spinel solids have a similar composition as compared with the unreacted slag system (Table 2). The slag contains a smaller amount of PbO in comparison with the composition of the original slag system. This can be ascribed to the reduction of PbO to Pb, followed by Pb evaporation.

Table 6 WDS analysis slag and spinel solids upper slag layer in $MgAl_2O_4$–slag sessile drop sample

Sample	Al_2O_3	MgO	'FeO'	Cu_2O	CaO	ZnO	PbO	SiO_2
Slag	12.37	0.5	8.1	1.49	11.5	2.7	29.1	36.1
Spinel	21.03	1	55	0.6	0	18.7	0	0.13

3.3.3 Influence interaction time on formation interaction layer $MgAl_2O_4$–slag

In the previous section, a clear interaction between the spinel substrate and the slag was demonstrated. Therefore, in addition to the spinel−slag sessile drop experiment, the interaction between spinel and slag was studied by immersing a $MgAl_2O_4$ substrate for different interaction time into the produced synthetic slag. An overview of the slag−$MgAl_2O_4$ interface evolution with the interaction time is shown in Fig. 9. After 10 s, a clear interaction layer is formed, as indicated in Fig. 9. This interaction layer grows with time. A steep increase in thickness of the interaction layer is noted during the first minutes while the increase in thickness between 1 and 3 min of interaction time is limited. In the first stage (after 30 s) an apparently quite dense interaction layer is formed. After 3 min, the upper part of the interaction layer seems to evolve to a layer with densely packed spinel particles and slag in between the spinel particles, similarly to the interaction layer present in the spinel−slag sessile drop sample.

WDS-line scans for each element across the interface were measured for the spinel samples after 10 s, 30 s and 3 min in the slag phase, as shown in Fig. 10. For each sample, the line-scans of the spinel forming elements (O, Al, Zn, Fe, Mg) and the main slag forming components (Ca, Cu, Pb, Si) have been grouped for convenience of comparison.

After 10 s, there is a delineated transition between the $MgAl_2O_4$ substrate and the slag phase. However, a slight enrichment of Fe could be noted at the interface, as indicated in Fig. 9. This enrichment in Fe was confirmed by a WDS-mapping of this specific region of the sample.

The line-scans of the samples obtained after 30 s show a more gradual transition between the $MgAl_2O_4$ and the slag. Based on the line scans, three different zones are distinguished. The first zone is unaffected $MgAl_2O_4$. The second zone is the interaction layer between the slag and the spinel substrate. For convenience, the lines that demarcate the interaction layer are defined to 90%−20% Al present in the $MgAl_2O_4$ substrate. The interaction layer consists mainly of spinel forming elements present in the substrate (Mg and Al) and the slag (Zn, Fe and Al). Self-evidently, the higher Mg and Al concentrations are found closest to the spinel substrate, while higher amounts of Fe and Zn are present closer to the slag. The slag forming elements (Ca, Cu, Pb and Si) are also found in very low amounts gradually increasing when coming closer to the slag. Finally, the third zone is the slag phase.

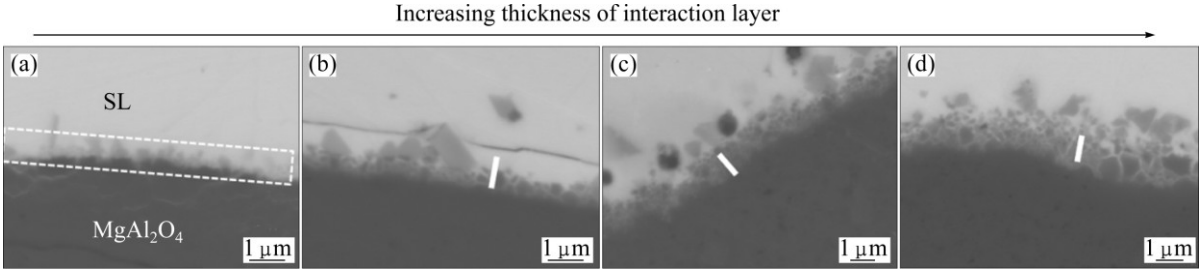

Fig. 9 BSE images illustrating interaction between $MgAl_2O_4$ substrate and slag after different interaction time (The white bars correspond to a distance of 1 μm): (a) 10 s; (b) 30 s; (c) 1 min; (d) 3 min

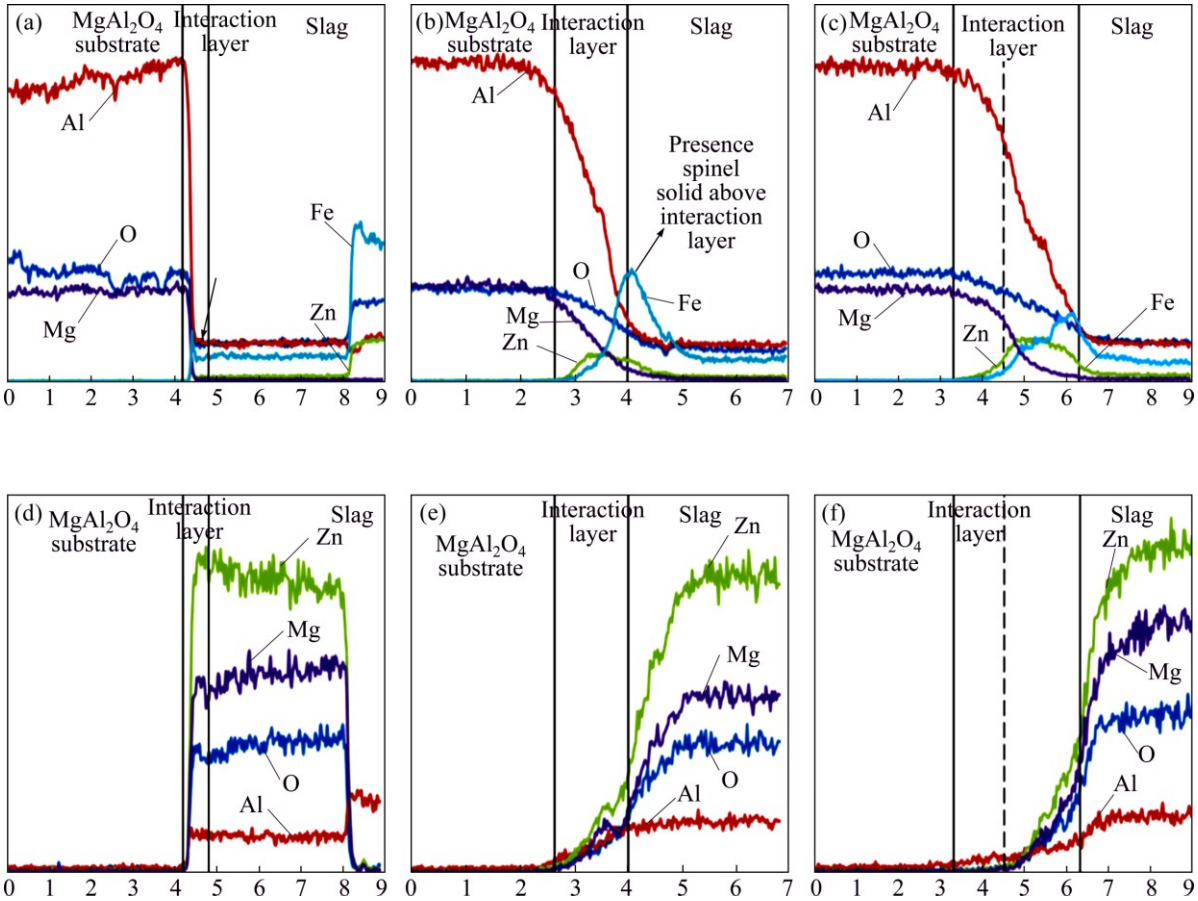

Fig. 10 Elemental WDS line scans of slag−$MgAl_2O_4$ interface after interaction time of 10 s (a, d), 30 s (b, e) and 3 min (c, f) (The upper graphs represent the compositional evolution at the interface for the spinel forming elements, the lower graphs show the evolution for the main slag forming elements)

The line-scans after 3 min display the same three layers. The interaction layer has thickened due to the prolonged interaction time and can be roughly subdivided into two zones. On one hand, next to the spinel substrate mainly spinel forming elements are present which give rise to the dense interaction layer next to the substrate. On the other hand, further away from the spinel substrate, both spinel forming elements and slag forming elements are present. This part of the interaction layer corresponds to the layer with densely packed spinel particles. Clearly, there is a large similarity between the structure of the interaction layer formed after 3 min of immersion and that of the interaction layer present after the sessile drop experiment (Fig. 7)

4 Discussion

4.1 $MgAl_2O_4$–slag interaction

The interaction between $MgAl_2O_4$ and slag has been studied in this work using two complementary experimental set-ups: a $MgAl_2O_4$−slag sessile drop experiment, studying the wetting behaviour, combined with a detailed microstructural investigation and by an immersion experiment of a spinel substrate in molten slag for different interaction time. In both experiments, a clear formation of an interaction layer at the interface of spinel and slag is observed.

Quantitative analysis of the interaction layer of the sessile drop sample demonstrated the presence of a $(Mg,Fe,Zn)(Al,Fe)_2O_4$ spinel-based interaction layer (Table 4) which consisted mainly of Al_2O_3 and MgO, combined with some ZnO and FeO from the slag. Here and in the remainder discussion, FeO corresponds to both FeO and Fe_2O_3. A gradient in the composition of the interaction layer was observed in both the sessile drop (Fig. 8) and the immersion experiment (Fig. 10). Closer to the $MgAl_2O_4$ substrate, mainly MgO and Al_2O_3 were present while closer to the slag FeO, ZnO and Al_2O_3 were observed. Al_2O_3 and MgO, originating from the $MgAl_2O_4$ substrate, were liberated and dissolved in the slag.

MgO was present throughout the whole slag droplet, with a maximum concentration in the slag near the interaction layer at the $MgAl_2O_4$−slag interface (Tables 4−6). Furthermore, MgO was also partially incorporated in spinel particles in both the upper and

lower slag layers. A significant increase of the Al_2O_3 content in the slag-phase in both the upper and lower slag layers compared with the unreacted slag is also observed.

Based on these observations, the following reaction is proposed to occur at the $MgAl_2O_4$−slag interface, which induces the formation of the observed interaction layer and causes the dissolution of MgO and Al_2O_3 in the slag:

$$MgAl_2O_4(s)+(Fe_2O_3,FeO, ZnO, Al_2O_3)(l, \text{in slag})\rightarrow (Mg^{2+}, Fe^{2+}, Zn^{2+})(Al^{3+}, Fe^{3+})_2O_4\ (s, \text{interaction layer})+MgO(l, \text{in slag})+Al_2O_3(l, \text{in slag}) \quad (1)$$

A similar interaction between $MgAl_2O_4$ and fayalitic slag has been observed by DONALD et al [21]:

$$FeO(l, \text{in slag})+MgAl_2O_4(s)\rightarrow (Mg_x^{2+}, Fe^{2+})Al_2^{3+}O_4 + Mg_{1-x}O(l, \text{in slag}) \quad (2)$$

Thermodynamic analysis of the slag–$MgAl_2O_4$ system has also been carried out using the FactSage thermochemical package (Fact and FT oxid database) in order to verify the proposed reaction scheme. The interaction between $MgAl_2O_4$ and the used synthetic slag (Table 1) has been simulated for the experimental conditions of the sessile drop experiment (1250 °C, p_{O_2}=7.5 Pa). 1 g of the targeted slag composition was taken as a starting point and different amounts of $MgAl_2O_4$ were added (up to 5 g). This variation in the amount of $MgAl_2O_4$ was applied to evaluating the formation of the interaction layer, depending on the local availability of MgO and Al_2O_3 from the $MgAl_2O_4$ spinel substrate. Figure 11 represents the variations of the fraction of spinel and slag, as a function of the amount of added $MgAl_2O_4$.

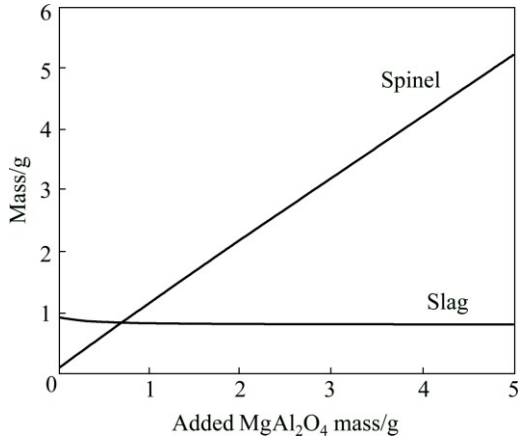

Fig. 11 Results of thermodynamic calculations, representing influence of addition of $MgAl_2O_4$ on amount of spinel and slag

The composition of the formed spinel solids, and thus the interaction layer, depends on the local availability of $MgAl_2O_4$ as seen in Fig. 12. An increase of the $MgAl_2O_4$ results in spinel solids with an increasing amount of MgO and Al_2O_3, which is found in the part of the interaction layer near the $MgAl_2O_4$ substrate in the experiments. When there is locally more slag present, FeO and ZnO will be more prominent in the formed spinel, which corresponds to the part of the interaction layer bordering on the slag liquid. These trends agree with the compositional variations throughout the formed interaction layers found in the experiment. The variation of the slag composition is shown in Fig. 12(b). The addition of $MgAl_2O_4$ results in an increase in the amount of MgO and Al_2O_3, as seen in Fig. 12. This affirms the experimentally observed liberation of MgO and Al_2O_3 into the slag. It can be observed that the addition of $MgAl_2O_4$ to slag generates more spinel in the system, which is likely to occur at the slag−$MgAl_2O_4$ interface resulting in an interaction layer. This indicates that there is a thermodynamic driving force for the formation of the interaction layer.

As stated in the previous paragraph, the thermodynamic condition for the formation of an interaction layer is satisfied. It is assumed that the

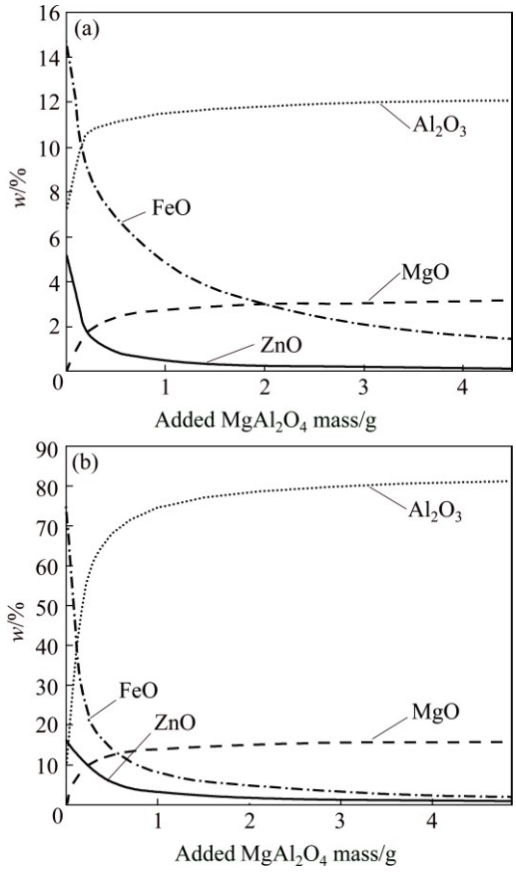

Fig. 12 Results of thermodynamic calculation by FactSage, representing influence of amount of $MgAl_2O_4$ on composition of spinel particles (a) and slag (b) (FeO corresponds to both FeO and Fe_2O_3. An excess of slag refers to the fact that more slag than $MgAl_2O_4$ is present, and an excess of $MgAl_2O_4$ refers to the fact that more $MgAl_2O_4$ than slag is present)

formation of this interaction layer occurs by nucleation and subsequent growth of the spinel particles.

SANDAHGE and YURUK [28] and LIU et al [29] proposed a four-step nucleation model of spinel particles at the MgO(solid)−CaO−SiO_2−Al_2O_3−(MgO) slag interface. Based on this model, it can be assumed that the nucleation of the spinel particles forming the interaction layer within our experimental systems involves a similar stepwise process: 1) the diffusion to the substrate and adsorption on the $MgAl_2O_4$ substrate of Zn, Fe, Al and O-bearing ions; 2) the break-up of any complex ions that may be involved on the surface; 3) surface diffusion of adsorbed ions and 4) collection of the critical concentration of Zn, Fe, Al, Mg and oxygen ions at nucleation sites with subsequent formation of nuclei of spinel [29]. It was observed that the interaction layer was already present after 10 s (Fig. 9). This indicates that the nucleation process must occur immediately after contact between the $MgAl_2O_4$ substrate and the slag.

The interaction layer displays a significant increase in thickness in the first minute. This fast formation rate of spinel particles has also been described before. NIGHTINGALE and MONAGHAN [30] investigated the dissolution of MgO and simultaneous formation of $MgAl_2O_4$ spinel solids in a slag containing CaO, Al_2O_3 and SiO_2. The formation of spinel crystals was observed within a few seconds. SCHEUNIS et al [31] studied the interaction between magnesia−chromite refractories and a spinel saturated PbO non-ferrous slag. The formation of a new $(Mg,Fe)(Al,Fe,Cr)_2O_4$ spinel layer at a growth rate of 290.5 $\mu m^2/h$ was observed. The extent to which the initially formed nuclei can grow depends on the relative fluxes of the FeO, ZnO, Al_2O_3 from the slag towards the $MgAl_2O_4$ substrate and the fluxes of MgO and Al_2O_3 away from the $MgAl_2O_4$ substrate. Due to the formation of the interaction layer, the slag near this interaction layer becomes locally depleted in the spinel forming oxides, which have to diffuse from the surrounding slag to the interaction layer to enable further growth. Dissolution of MgO and Al_2O_3 from the spinel substrate into the slag is assumed to occur from the initial stage onwards, although it is inhibited by the formation of the interaction layer. If a continuous interaction layer is formed, MgO and Al_2O_3 originating from the $MgAl_2O_4$ substrate can continue to dissolve based on an indirect dissolution process, as described by LIU et al [29].

Longer interaction time also results in a change in structure of the interaction layer, as seen in Fig. 9. After 30 s, the spinel layer consists of a very dense spinel layer, while after 1 min the upper part of the interaction layer consists of separate spinel particles which are densely packed. This can be on one hand linked to the relatively lower spinel formation rate due to the depletion of the spinel forming elements. On the other hand, it is also possible that some sort of dissociation occurs at the interaction layer–slag interface [29].

Based on the experimental observations of the chemical processes occurring at the interface (Eq. (1)), the diffusion and dissolution of MgO and Al_2O_3 originating from the spinel substrate in the slag and the nucleation and formation kinetics of the spinel, a schematic representation of the interaction layer formation at the $MgAl_2O_4$−slag interface for the applied system is proposed in Fig. 13. For this purpose, the time as observed during the immersion experiment was used. Hereby the interaction layer ($(Mg, Fe, Zn)(Al, Fe)_2O_4$) formed immediately from the first moment of contact between the $MgAl_2O_4$ spinel substrate and the slag. The interaction layer indeed nucleates and grows significantly in the first seconds, after which stagnation in the growth of the interaction layer is observed, probably due to a local depletion in spinel forming elements. This formation of the interaction layer was combined with the dissolution and diffusion of MgO and Al_2O_3 in the slag phase.

4.2 Comparison wetting behaviour copper and slag on spinel

A significant difference is noted between the

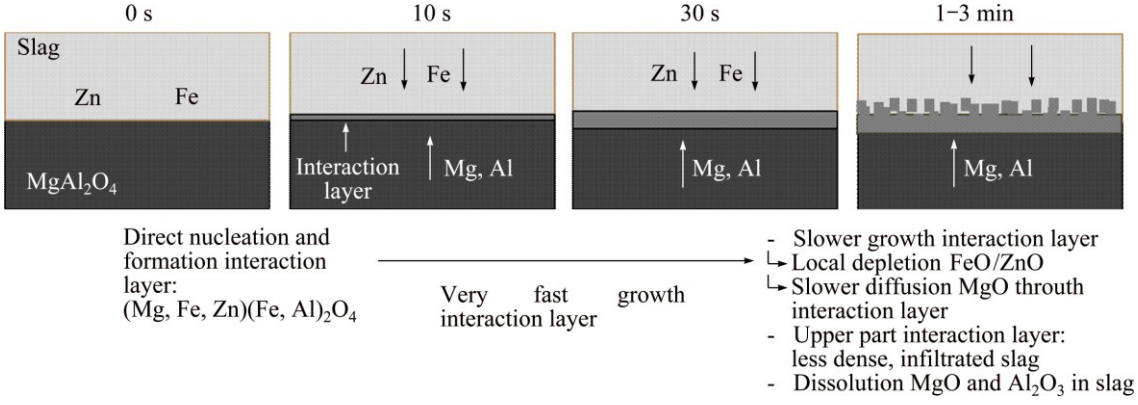

Fig. 13 Proposed mechanism for slag and $MgAl_2O_4$ interaction

wetting behaviour of copper and slag on $MgAl_2O_4$. The synthetic slag displayed a very good wetting behaviour on $MgAl_2O_4$ (Figs. 4 and 5), having big similarity with the kinetics of reactive wetting, as described by EUSTATHOPOULOS et al [15] and the reactive wetting between $MgAl_2O_4$ and $CaO-Al_2O_3-SiO_2-MgO$ slags as observed by ABDEYAZDAN et al [20]. Namely a rapid decrease of the contact angle at first, reaches a plateau after longer time. It should, however, be noted that both EUSTATOPOULOS et al [15] and ABDEYAZDAN et al [20] added the slag on the substrate at high temperature, while in our set-up the droplet melts at lower temperature and then further heats together with the substrate. This difference in experimental set-up explains the difference in timescale with the results of ABDEYAZDAN et al [20], who observed a rapid decrease of the contact angle within 10 s, as compared to 200 s in our slag−$MgAl_2O_4$ sessile drop experiment. The assumption of reactive wetting for the spinel−slag case was confirmed by microstructural analysis clearly showing the presence of an interaction layer. However, the decrease of the contact angle, shown in Fig. 5, is therefore assumed to be mainly attributed to the reaction and not due to the increase in temperature.

By contrast, copper displayed a non-wetting behaviour, with an average contact angle of 103°. Based on the BSE image of the copper−spinel interface, no chemical interaction was noted between the two phases. Similar non-wetting behaviour between spinel particles and Cu−Ag alloys was observed for different oxygen partial pressures (10^{-8}–10^{-3} Pa) in our previous work [13]. The comparison between the wetting behaviour of copper on $MgAl_2O_4$ and $ZnFe_2O_4$ revealed a better wetting of the $ZnFe_2O_4$ substrate, indicating the importance, among others, of the chemical composition of the spinel substrate [26]. However, to our knowledge, no experimental data have been published, showing a comparable good wetting behaviour as slag on spinel. According to Ref. [15], the lowest experimental observed contact angle between magnetite and copper was around 60°, with an estimated oxide dissolution of a mole fraction of 10^{-3} in the liquid metal.

Based on the obtained results, it would be expected that a copper droplet would not be able to attach to a spinel solid which is surrounded by slag as the spinel−copper interfacial tension appears to be less beneficial than the spinel−slag interfacial tension, although sticking droplets are observed in industrial slags. However, attached droplets have been observed in our previous work. It has been derived that the attachment to spinel particles is energetically favourable if the following condition is valid [32]:

$$\gamma_{Sl-Cu}+\gamma_{Sp-Sl}\geq\gamma_{Sp-Cu} \quad (3)$$

where γ_{Sl-Cu} is the slag−copper interfacial tension, γ_{Sp-Sl} is the spinel−slag interfacial tension and γ_{Sp-Cu} is the spinel−copper interfacial tension.

It is possible that the performed sessile drop experiments, making use of a protective argon atmosphere, are not representative for the system of sticking droplets in industrial or synthetic slag system. This can be attributed to a difference in the interfacial energies between the slag and copper droplets or spinel particles compared with the interfacial energies between argon and the copper droplet or $MgAl_2O_4$ substrate. However, the interactions at the spinel−slag interface, which are believed to be responsible for the good wettability observed in these experiments, will also take place in industrial slag systems. Thus, based on the current experiment, we can expect that the wetting of spinel by copper droplets is more difficult than the wetting of spinel by slag, also in industrial slag systems.

With this, it can be assumed that other mechanisms than interfacial tension most probably have an important role in the phenomenon of sticking droplets. The latter is enforced by observations in our previous work [32] and by phase field simulations performed by BELLEMANS et al [33]. They studied the attachment of metallic droplets to solid particles in liquid slags with a phase field model, in which the influence of particle characteristics (the particle density, perimeter, shape and distribution) were studied for systems of high and low wettability of the metallic phase. Based on the comparison of the modelled results and experimental results using the similar synthetic slag system as in this work, a low wettability system showed the best similarity, and thus the attachment is believed to partly originate from reactions among the metal, the slag and the solid particles. Based on experimental results in our previous work, similar conclusions were formulated [32]. However, more experimental research is necessary to give a decisive answer whether other mechanisms than interfacial tension are responsible for the occurrence of copper alloy droplets sticking to spinel particles.

5 Conclusions

1) Copper displayed a non-wetting behaviour on $MgAl_2O_4$, and no chemical interactions were observed between these phases. Slag, on the other hand, displayed a reactive wetting on $MgAl_2O_4$ substrates, and an interaction layer is formed at the interface. This interaction layer consisted of (Mg, Fe, Zn)(Al, Fe)$_2O_4$ spinel. Its nucleation and formation was very fast as indicated by samples with a 10 s interaction time. Subsequently, the formation speed lowered. Next to the formation of spinel layer, the diffusion of MgO and Al_2O_3 from the spinel substrate into the slag droplets was

also noted.

2) Based on the current results showing that the wetting of slag on spinel is much better than the wetting of copper on spinel, it can be concluded that attached copper droplets are not stable or that there is at least a mechanical barrier of slag for copper droplets to overcome in order to attach to spinel solids present in the slag. Additionally, it is suggested that other processes, such as chemical reactions, probably play an important role in the origin of droplets sticking to spinel particles in the slags.

Acknowledgments

The authors wish to thank the agency for innovation by science and technology in Flanders (IWT, project 110541) and Umicore for its financial support and in particular Maurits van Camp, Luc Coeck, Saskia Bodvin, Kristel Van Ostaeyen, Eddy Boydens, Danny Leysen and the technical staff of Umicore R&D for their support with the experiments and characterization. Pieter L'Hoëst is acknowledged for the help with the EPMA-WDS analysis and Joris Van Dyck and Jeroen Heulens for the help with the sessile drop experiments.

References

[1] DEGEL R, OTERDOOM H, KUNZE J, WARCZOK A, RIVEROS G. Latest results of the slag cleaning reactor for copper recovery and its potential for the PGM industry [C]//Proceedings of Conference of Third International Platinum Conference "Platinum in Transformation". Sun City, South Africa: The Southern African Institute of Mining and Metallurgy, 2008: 197−202.

[2] JONG-LENG L, JUUSELA M, GRAY N B, SUTALO I D. Entrainment of a two-layer liquid through a taphole [J]. Metallurgical and Materials Transactions B (Process Metallurgy and Materials Processing Science), 2003, 34B: 821−832.

[3] SUH I K, WASEDA Y, YAZAWA A. Some interesting aspects of non-ferrous metallurgical slags [J]. High Temperature Materials and Processes, 1988, 8: 65−88.

[4] CARDONA N, HERNANDEZ L, ARANEDA E, PARRA R. Evaluation of copper losses in the slag cleaning circuits from two Chilean smelters [C]// Proceedings of Conference of Copper 2010. Hamburg, Germany: GMDB, 2010: 2637−2654.

[5] SRIDHAR R, TOGURI J, SIMEONOV S. Copper losses and thermodynamic considerations in copper smelting [J]. Metallurgical and Materials Transactions B, 1997, 28: 191−200.

[6] IMRIS I, SANCHEZ M, ACHURRA G. Copper losses to slags obtained from the El Teniente process [C]// Proceedings of 7th International Conference on Molten Slags, Fluxes and Salts. Johannesburg, South Africa: The South African Institute of Mining and Metallurgy, 2004: 177−182.

[7] CARDONA N, COURSOL P, MACKEY P J, PARRA R. Physical chemistry of copper smelting slags and copper losses at the Paipote smelter. Part 1 — Thermodynamic modelling [J]. Canadian Metallurgical Quarterly, 2011, 50: 318−329.

[8] IP S W, TOGURI J M. Entrainment behavior of copper and copper matte in copper smelting operations [J]. Metallurgical Transactions B —Process Metallurgy, 1992, 23: 303−311.

[9] MINTO R, DAVENPORT W G. Entrapment and flotation of matte in molten slags [J]. Canadian Mining and Metallurgical Bulletin, 1972, 65: C36−42.

[10] MARU H C, WASAN D T, KINTNER R C. Behavior of a rigid sphere at a liquid-liquid interface [J]. Chemical Engineering Science, 1971, 26: 1615−1628.

[11] ANDREWS L. Base metal losses to furnace slag during processing of platinum-bearing concentrates [D]. Pretoria: Environment and Information Technology, University of Pretoria, 2008: 19−28.

[12] MALFLIET A, LOTFIAN S, SCHEUNIS L, PETKOV V, PANDELAERS L, JONES P T, BLANPAIN B. Degradation mechanisms and use of refractory linings in copper production processes: A critical review [J]. Journal of the European Ceramic Society, 2014, 34: 849−876.

[13] de WILDE E, BELLEMANS I, CAMPFORTS M, KHALIQ A, VANMEENSEL K, SEVENO D, GUO M, RHAMDHANI M, BROOKS G A, BLANPAIN B, MOELANS N, VERBEKEN K. Wetting behaviour of Cu based alloys on spinel substrates in pyrometallurgical context [J]. Materials Science and Technology, 2015.

[14] EUSTATHOPOULOS N, DREVET B. Determination of the nature of metal-oxide interfacial interactions from sessile drop data [J]. Materials Science and Engineering A — Structural Materials Properties Microstructure and Processing, 1998, 249: 176−183.

[15] EUSTATHOPOULOS N, NICHOLAS M G, DREVET B. Wettability at high temperatures [M]//Pergamon: Materials Series, 1999: 420.

[16] ZHANG D, ZHU D Y, ZHANG T, WANG Q F. Kinetics of reactive wetting of graphite by liquid Al and Cu−Si alloys [J]. Transactions of Nonferrous Metals Society of China, 2015, 25: 2473−2480.

[17] HEO S H, LEE K, CHUNG Y. Reactive wetting phenomena of MgO−C refractories in contact with CaO−SiO_2 slag [J]. Transactions of Nonferrous Metals Society of China, 2012, 22(S3): s870−s875.

[18] KOZLOVA O B, SUVOROV S A. The wetting of refractories of the MgO−Al_2O_3−ZrO_2 system with metal melts [J]. Refractories, 1976, 17: 763−767.

[19] FUKAMI N, WAKAMATSU R, SHINOZAKI N, WASAI K. Wettability between porous $MgAl_2O_4$ substrates and molten iron [J]. Materials Transactions, 2009, 50: 2552−2556.

[20] ABDEYAZDAN H, DOGAN N, RHAMDHANI M, CHAPMAN M, MONAGHAN B. Dynamic wetting of CaO−Al_2O_3−SiO_2−MgO liquid oxide on $MgAl_2O_4$ spinel [J]. Metallurgical and Materials Transactions B — Process Metallurgy and Materials Processing Science, 2014, 46: 208−219.

[21] DONALD J R, TOGURI J M, DOYLE C. Surface interactions between fayalite slags and synthetic spinels and solid solutions [J]. Metallurgical and Materials Transactions B—Process Metallurgy and Materials Processing Science, 1998, 29: 317−323.

[22] TRAN T, XIE D, CHENG Y B. Effects of slag chemistry and temperature on wetting and penetration of refractories by slags [C]//VII International Conference on Molten Slags Fluxes and Salts, The South African Institute of Mining and Metallurgy, 2004.

[23] de WILDE E, BELLEMANS I, VERVYNCKT S, CAMPFORTS M, VANMEENSEL K, MOELANS N, VERBEKEN K. Towards a methology to study the interaction between Cu droplets and spinel particles in slags [C]//European Metallurgical Conference. Weimar: GDMB, 2013: 161−174.

[24] DE WILDE E, VERVYNCKT S, CAMPFORTS M, GODIER G, VANMEENSEL K, MOELANS N, VERBEKEN K. Characterization methodology for copper-droplet losses in slags copper conference. Santiago, 2013: 189−197.

[25] BELLEMANS I. Towards a methodolgy to study the interaction between Cu droplets and spinels [D]//Ghent, Belgium: Materials Science and Engineering, Ghent University, 2013: 184.

[26] de WILDE E, BELLEMANS I, CAMPFORTS M, GUO M, VANMEENSEL K, BLANPAIN B, MOELANS N, VERBEKEN K.

Wetting behaviour of spinel with copper to understand metallic copper losses to slags [C]//European Metallurgical Conference. Düsseldorf: GDMB, 2015: 3−18.

[27] STALDER A F, MELCHIOR T, MULLER M, SAGE D, BLU T, UNSER M. Low-bond axisymmetric drop shape analysis for surface tension and contact angle measurements of sessile drops [J]. Colloids and Surfaces A—Physicochemical and Engineering Aspects, 2010, 364: 72−81.

[28] SANDHAGE K H, YUREK G J. Indirect dissolution of sapphier into silicate melts [J]. Journal of the American Ceramic Society, 1988, 71: 478−489.

[29] LIU J, GUO M, JONES P T, VERHAEGHE F, BLANPAIN B, WOLLANTS P. In situ observation of the direct and indirect dissolution of MgO particles in $CaO-Al_2O_3-SiO_2$-based slags [J]. Journal of the European Ceramic Society, 2007, 27: 1961−1972.

[30] NIGHTINGALE S A, MONAGHAN B J. Kinetics of spinel formation and growth during dissolution of MgO in $CaO-Al_2O_3-SiO_2$ slag [J]. Metallurgical and Materials Transactions B—Process Metallurgy and Materials Processing Science, 2008, 39: 643−648.

[31] SCHEUNIS L, CAMPFORTS M, JONES P T, BLANPAIN B, MALFLIET A. The influence of slag compositional changes on the chemical degradation of magnesia-chromite refractories exposed to PbO-based non-ferrous slag saturated in spinel [J]. Journal of the European Ceramic Society, 2015, 35: 347−355.

[32] de WILDE E, BELLEMANS I, ZHENG L, CAMPFORTS M, GUO M, BLANPAIN B, MOELANS N, VERBEKEN K. Origin and sedimentation characteristics of sticking copper droplets to spinel solids in pyrometallurgical slags [J]. Metallurgical and Materials Transactions B, 10.1080/02670836.2016.1151998.

[33] BELLEMANS I, de WILDE E, MOELANS N, VERBEKEN K. Phase field modelling of the attachment of metallic droplets to solid particles in liquid slags: Influence of particle characteristics [J]. Acta Materialia, 2015, 101: 172−180.

采用静滴法评估高温铜/尖晶石和炉渣/尖晶石的交互作用

E. de WILDE[1], I. BELLEMANS[1], M. CAMPFORTS[2], M. GUO[3],
B. BLANPAIN[3], N. MOELANS[3], K. VERBEKEN[1]

1. Department of Materials Science and Engineering, Ghent University,
Technologiepark 903, B-9052 Zwijnaarde (Ghent), Belgium;
2. Umicore R&D, Kasteelstraat 7, B-2250 Olen, Belgium;
3. Department of Materials Engineering, KU Leuven, Kasteelpark Arenberg 44, bus 2450,
B-3001 Heverlee (Leuven), Belgium

摘　要：在冶金炉渣中，依附在固体尖晶石上的金属熔滴可有效阻止铜在炉渣中的沉积。为了理解这一现象，评估了尖晶石颗粒和铜及与炉渣的交互作用。分别以 $PbO-FeO-SiO_2-CaO-Al_2O_3-Cu_2O-ZnO$ 合成炉渣、纯铜和 $MgAl_2O_4$ 基体代表工业废渣、铜滴和固体尖晶石。用静滴法和显微组织分析研究铜−$MgAl_2O_4$ 和炉渣−$MgAl_2O_4$ 交互作用。另外，采用沉浸实验研究时间对炉渣−$MgAl_2O_4$ 交互作用的影响。结果表明，铜在 $MgAl_2O_4$ 上不润湿，然而炉渣在 $MgAl_2O_4$ 上润湿并在界面处形成了$(Mg, Fe, Zn)(Al, Fe)_2O_4$ 尖晶石交互层，在浸出实验中也观察到了该现象。同时观察到了 MgO 和 Al_2O_3 从尖晶石基体扩散到炉渣中。

关键词：静滴法；铜；尖晶石；炉渣

(Edited by Xiang-qun LI)